Experimental Studies on the Relaxation Behavior of Commercial Polymer Melts

Yurun Fan,[1] Huayong Liao[1,2]

[1]*State Key Laboratory of Fluid Power Transmission and Control, Zhejiang University, Hangzhou 310027, China*
[2]*Polymer Materials Key Laboratory of Changzhou City, Jiangsu Polytechnic University, Changzhou 213164,China*

Received 27 December 2007; accepted 21 March 2008
DOI 10.1002/app.28558
Published online 23 July 2008 in Wiley InterScience (www.interscience.wiley.com).

ABSTRACT: With a rotary rheometer, various methods were used to determine the characteristic relaxation times for a commercial polydimethylsiloxane (PDMS), and their consistency and relation to the linear relaxation spectrum were examined. The experimental damping functions of the step deformation of the PDMS, a polymethylvinylsiloxane, and a high-density polyethylene were compared with predictions of the Doi–Edwards theory and Marrucci model; the effect of wall slip on the damping function data is discussed, and the appearance of stress peaks due to material instability as the strain increased above a critical value is detailed. Through the application of a previously proposed stress decomposition method to the data of large-amplitude oscillatory shear for the PDMS sample, the relationship between the generalized elastic modulus $[G'_N(\omega,\gamma)]$ and the shear relaxation modulus $[G(\gamma,t)]$ was investigated. In the linear and initial nonlinear regimes, as the angular frequency (ω) increased, $G'_N(\omega,\gamma)$ approached $G(\gamma,t)$ on the timescale $t = 1/\omega$, where t is the time. © 2008 Wiley Periodicals, Inc. J Appl Polym Sci 110: 1520–1530, 2008

Key words: melt; polyethylene (PE); relaxation; rheology; viscoelastic properties

INTRODUCTION

Relaxation time plays a central role in polymer rheology. For polymers of narrow molecular weight distribution, the boundary between the plateau and terminal zones of the linear relaxation modulus $[G(t)]$ is rather sharp,[1] and the existence of a single terminal relaxation time is clear. For low-molecular-weight polymers, this corresponds to the Rouse time: $\tau_R = \frac{6\eta_0 M}{\pi^2 \rho RT}$, where M is the average molecular mass, η_0 is the zero-shear viscosity, ρ is the density, R is the gas constant, and T is the absolute temperature.[2] For high-molecular-weight polymers ($M >$ 35,000 Da), the terminal relaxation time corresponds to the chain disengagement time (τ_d; or reptation time), which is estimated to be $\tau_d = \frac{12\eta_0}{\pi^2 G_N^0}$, where G_N^0 is the plateau modulus.[3,4] For most commercial polymers, a wide distribution of molecular weight broadens the crossover from the terminal zone to the plateau zone, and a continuous or discrete spectrum is necessary to precisely describe their complex relaxation behaviors. However, to simplify modeling and numerical simulation, there are various experimental methods available to determine a characteristic time that can represent the major physical process of interest. A convenient method is to use the crossover frequency (ω_c) of the dynamic moduli $[G'(\omega)$ and $G''(\omega)]$ in the small-amplitude oscillatory shear (SAOS) and the critical shear rate $\dot{\gamma}_c$ for the onset of shear thinning in steady shear flow.[5] For monodisperse systems, shear thinning occurs at $\dot{\gamma}_c \cong 1/\tau_d$.[3] The two characteristic times are related by $\tau_d = \alpha/\omega_c = \alpha\tau_c$, where τ_c is the crossover time, α is an inherent constant of the polymer sample; for an isotropic polypropylene with a polydispersity index of 4.1, Elmoumni et al.[5] reported $\alpha \approx 8$. Another way to determine a characteristic relaxation time is to use the creep-recovery test or SAOS. In the uncorrelated drag model of Graessley,[2,6] the weight-average relaxation time (τ_w) for a narrow distribution of relaxation times in the terminal zone is given by $\tau_w = \eta_0 J_e^0$, where J_e^0 is the steady-state shear compliance, which can be measured by creep recovery or SAOS at low frequencies.[2,6] In the framework of the tube reptation model, the longest relaxation time for the reptation process is given by

$$\tau_d = (10/\pi^2)\eta_0 J_e^0 \quad (1)$$

which is identical to τ_w for monodisperse polymers.

In this study, we used a variety of the aforementioned methods to determine the characteristic times

Correspondence to: Y. Fan (yurunfan@zju.edu.cn).
Contract grant sponsor: National Natural Science Foundation of China; contract grant number: 10472105.
Contract grant sponsor: Special Fund of Ministry of Education of China; contract grant number: 20050335050.

of a commercial polydisperse polydimethylsiloxane (PDMS) and to examine their relation to the linear relaxation spectrum.

The damping function [$h(\gamma)$] of the relaxation modulus is a crucial test for the evaluation of constitutive equations of polymer melts. The published data on $h(\gamma)$ were well reviewed by Osaki[7] and are classified into three types: the normal exponential type, the power law, and the kinked type. Generally, for monodisperse polymers, the theory of Doi and Edwards[3] and the model proposed by Marrucci et al.[8] give good predictions of $h(\gamma)$ and the normal stress ratio. Iza and Bousmina[9] studied the $h(\gamma)$'s of several polymers with polydispersity indices from 1.09 to 2.45; within a strain range of 0.01–5, better prediction with the Marrucci model than with the Doi–Edwards theory was observed. However, as the strain magnitude increased, experiments of step deformation often confront a serious problem; that is, a wall slip may set in and make the true strain (γ) considerably lower than the apparent one,[10] or stratified deformations (shear banding) may take place in the bulk of sample;[11] in some cases, these two phenomena are hard to distinguish from each other. Archer et al.[12] observed apparent slip within a few micrometers on a glass surface with tracers suspended in a highly entangled polystyrene solution. A nonlinear velocity profile was observed by Tapadia and Wang[13,14] for an entangled polybutadiene solution in the gap of a cone-and-plate fixture when it was sheared in the stress plateau region with particle-tracking velocimetry; also, a shear banding phenomenon was observed under oscillatory shearing with large amplitudes when the imposed frequency was higher than the aforementioned ω_c.

In this article, we report the results of step strain experiments for three polymer samples: a PDMS, a polymethylvinylsiloxane (PMVS), and a high-density polyethylene (HDPE) with the polydispersity indices ranging from 1.5 to 6.1. We compared the obtained $h(\gamma)$'s with the theoretical predictions, examined the effect of the uncertain γ on $h(\gamma)$, and detailed the appearance of stress peaks as the strain increased, which was predicted by material instability theory.[3,11,15]

In the linear viscoelastic regime, both $G(t)$ and $G'(\omega)$ are a measure of elastic energy, and it is well established that as $G(t)$ approaches the plateau region, its value is equal to $G'(\omega)$ on the timescale $t = 1/\omega$, where t is the time and ω is the angular frequency.[2] This relation is useful for obtaining $G(t)$ at very short time intervals because, for polymers such as PDMS, it difficult to directly measure $G(t)$ near the plateau region because of instrumental limitation of temperature control and the rising time in step deformation. The desired data can be replaced by $G'(\omega)_{\omega=1/t}$ with an acceptable error.[16] Beyond the linear viscoelastic regime, however, the $G'(\omega)$ and $G''(\omega)$ reported by the rheometer lose their usual physical meaning. Large-amplitude oscillatory shear (LAOS) is an important tool for analyzing the nonlinear behavior of complex fluids.[14,17,18] Recently, Cho et al.[19] proposed a method to decompose the nonlinear stress response in LAOS into elastic and viscous components on the basis of the geometric aspect of viscoelasticity. In the last part of this article, by applying the method of Cho et al. to the LAOS experiment for PDMS, we compare the generalized elastic modulus with the shear relaxation modulus [$G(\gamma,t)$] at large strains and find a similar relation to that in the linear viscoelastic regime.

TABLE I
Molecular Parameters of the Polymers

Polymer	M_n	M_w	M_w/M_n
PDMS 101	4.9×10^5	7.3×10^5	1.5
PMVS110-2	3.7×10^5	5.7×10^5	1.6
HDPE 5306J	1.5×10^4	9.4×10^4	6.1

M_n, number-average molecular weight.

EXPERIMENTAL

Materials

Three polymer samples were used in this study: PDMS 101 and PMVS 110-2, both manufactured by Jilin Jihui Industry and Commerce Co., Ltd. (Jilin, China) and HDPE 5306J, manufactured by Yangzi Petroleum Co., Ltd. (Shanghai, China). Table I lists the molecular weights measured with gel permeation chromatography. HDPE sample disks 20 mm in diameter were prepared by molding with a laboratory press at 150°C and under 10 MPa for 10 min; they were then cooled in the atmosphere.

Rheometry

The experiments were done on a Gemini 200 rotary rheometer manufactured by Bohlin Instruments Co. Almost all of the rheological experiments were done with parallel plates 15 mm in diameter with a gap of 0.5 mm. Parallel plates with a diameter of 25 mm and a gap of 1.21 mm were used in the line-marker experiment to clearly show the wall slip effect. Before the experiments, the plates were cleaned carefully with acetone to eliminate possible contaminants and residual polymer chains.

Temperature control

The main experimental temperatures were 40, 40, and 150°C for the PDMS, PMVS, and HDPE samples, respectively. Before rheological measurement, there was about 5 to 10 min when the sample disk

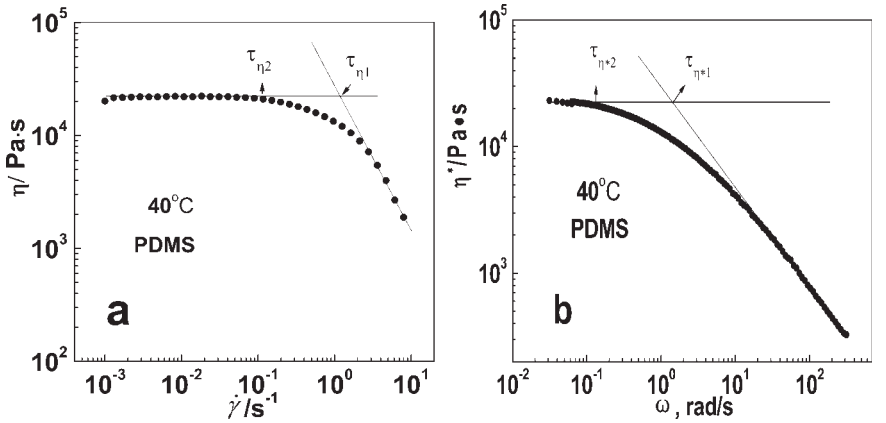

Figure 1 Shear viscosity versus the (a) shear rate in steady shear and (b) angular frequency in dynamic shear for PDMS at 40°C, from which $\tau_{\eta 1}$ was determined by the crossover of the zero-shear plateau and shear-thinning slope, $\tau_{\eta 2}$ was determined by the onset of shear thinning behavior.

was first melted in the rheometer at the required temperature to remove the thermal and strain history. During the experiments, the temperature fluctuation did not exceed ±0.2°C.

RESULTS AND DISCUSSION

Relaxation times of PDMS

Determination of the relaxation time by shear thinning

In steady shear flow, shear thinning occurs at $\dot{\gamma} \cong 1/\tau_d$, where $\dot{\gamma}$. is the shear rate and τ_d is the disentanglement time in tube theory.[3] The corresponding characteristic relaxation time ($\tau_{\eta 1}$) of PDMS in steady shear flow can be estimated by $\tau_{\eta 1} = 1/\dot{\gamma}_{\eta 1}$, where $\dot{\gamma}_{\eta 1}$ is the shear rate at which the zero-shear plateau and shear thinning slope cross, or by $\tau_{\eta 2} = 1/\dot{\gamma}_{\eta 2}$, where $\dot{\gamma}_{\eta 2}$ is the shear rate at which the shear thinning behavior occurs at the very beginning.[20] Similar definitions were used for the small-amplitude oscillation test by replacement of the shear rate with ω and the steady viscosity with the dynamic one, as shown in Figure 1. The obtained relaxation times are listed in Table II, in which $\tau_{\eta 2}$ seemed to give the more consistent results of the two methods.

Determination of the relaxation time by the creep-recovery test

The weight-average relaxation time $\tau(_w)$ (or the longest τ_d) was determined by the creep-recovery test and with eq. (1). The experimental curves for the PDMS sample are shown in Figure 2. Table III lists the results from three runs; the repeatability was good. The average relaxation time was 8.0 s, which agreed well with that determined by the shear thinning tests. Additionally, with the cone and plate with a diameter of 25 mm and a cone angle of 5.4°, $\tau_d = 7.0$ s was obtained.

TABLE II
Relaxation Times of PDMS at 40°C Estimated from the Steady and Linear Dynamic Viscosities

Test mode	$\tau_{\eta 1}$ (s)	$\tau_{\eta 2}$ (s)
Steady shear	0.84	8.6
Dynamic shear	0.70	8.2

Linear relaxation spectrum

SAOS experiments were done for the PDMS sample at four temperatures: 20, 40, 60, and 80°C. The controlled shear stress (τ) was 100 Pa (in the linear region). Up and down frequency sweeps gave almost identical curves. The G_N^0 obtained was 2.3 × 10^5Pa, compared with a value of 2.4 × 10^5 Pa from the literature;[11] the complex zero-shear viscosity (η_0*) was 2.3 × 10^4 Pa s at 40°C, which agreed with η_0 measured by the creeping test. A master curve (shifted to 40°C) was obtained by time–temperature

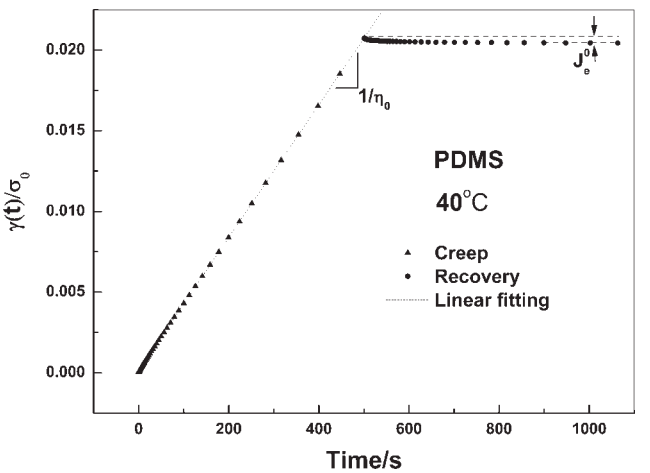

Figure 2 Creep-recovery test for PDMS at 40°C with the shear stress (σ_0) = η_0 is the zero-shear viscosity. 500 Pa imposed for 500 s and a recovery time of 500 s.

TABLE III
Creep-recovery Test Data for PDMS at 40°C

	Run			
	1	2	3	Average
J_e^0 (1/Pa)	3.4×10^{-4}	3.0×10^{-4}	3.3×10^{-4}	3.2×10^{-4}
η_0 (Pa s)	2.44×10^4	2.45×10^4	2.43×10^4	2.44×10^4
τ_d (s)	8.4	7.5	8.1	8.0

superposition, as shown in Figure 3, with the Arrhenius type shift factor (α_T):

$$\alpha_T = K_1 e^{E/RT} \tag{2}$$

where K_1 is a material constant and is 1.79×10^{-3}; E is the activation energy and is 16.5 kJ/mol, which is very close to the 16.7 kJ/mol reported in the literature;[21] and $R = 8.3145$ J/K·mol. Notice that the crossover time $1/\omega_c$ is 0.3 s at 40°C. Thus, with $\tau_d = 8.0$ s derived from the creep-recovery test, $\tau_d = 27/\omega_c = 27\tau_c$ for this PDMS sample.

In our step-strain experiments, the time lapse required to reach the target strain was limited by 20 ms in the linear region and by 45 ms for large strains. Because the rheometer we used was not able to run below room temperature, it was difficult to obtain the data of $G(t)$ near the plateau region of the PDMS sample. The material response in step deformation was elastic in nature, so $G(t)$ and $G'(\omega)$ were mirror images at short timescales,[2,16] that is,

$$\lim_{t\to 0} G(t) = \lim_{\omega\to\infty} G'(\omega) \tag{3}$$

This limiting relation was valid, as illustrated in Figure 4, where the two responses became close to each other (within 5% error) at times shorter than 45 ms.

The relaxation behavior of PDMS could be more precisely described by a discrete spectrum of N relaxation times (τ_i's) and the corresponding spectral strength (g_i):[2,22]

$$G(t) = \sum_{i=1}^{N} g_i e^{-t/\tau_i} \tag{4}$$

We obtained the parameters g_i and τ_i by fitting the measured $G(t)$ and the extrapolated $G(t) = G'(\omega)_{\omega=1/t}$ when $t < 20$ ms by using the nonlinear curve-fitting tool of the software Origin7.0 (Origin Lab Co., Northampton, MA). The results are listed in Table IV. Given the relaxation spectrum, the dynamic moduli could be calculated as follows:[16,23]

$$G'(\omega) = \sum_{i=1}^{N} \frac{g_i \tau_i^2 \omega^2}{1 + \tau_i^2 \omega^2} \tag{5}$$

$$G''(\omega) = \sum_{i=1}^{N} \frac{g_i \tau_i \omega}{1 + \tau_i^2 \omega^2} \tag{6}$$

Figure 5 compares the calculated moduli with the experimental data extracted from the master curves of Figure 3(a). The predictions were good, especially at low frequencies.

Step shear deformation of large strains

Damping function

In linear viscoelastic regime, the shear relaxation moduli are independent of the strains. In the nonlinear regime, the conventional log–log relaxation curves are nearly parallel after a certain initial time, which means that the shear relaxation modulus could be separated into time- and strain-dependent factors:[7,23]

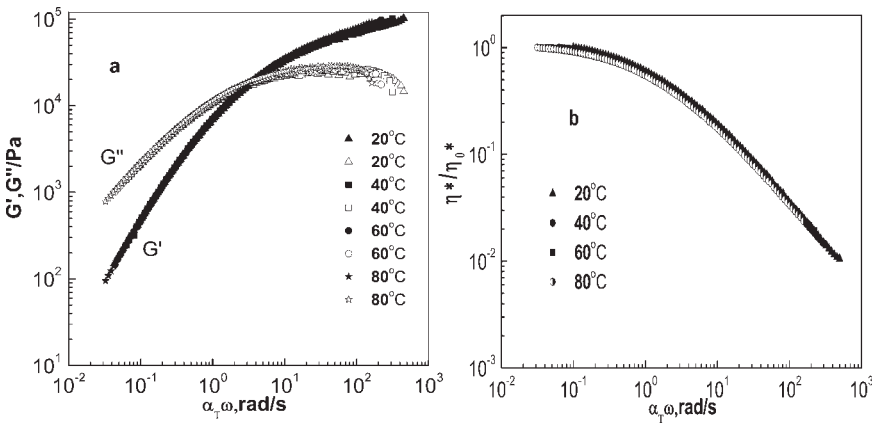

Figure 3 Master curves of (a) the loss and storage moduli and (b) the complex viscosity of PDMS at 40°C.

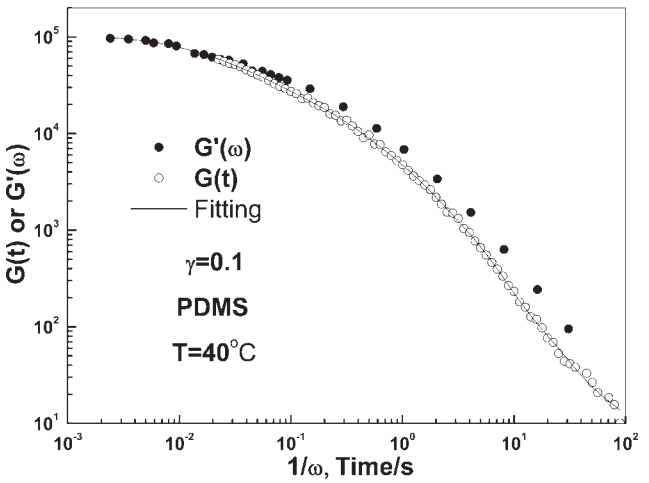

Figure 4 Linear stress-relaxation data of PDMS at 40°C and the fitting curve plotted with nonlinear regression.

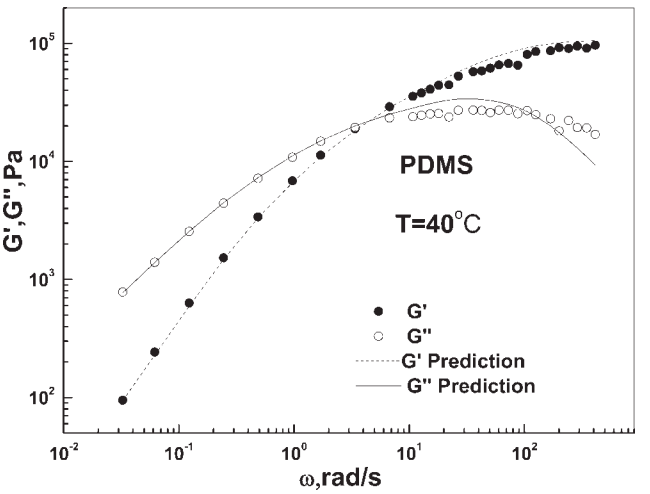

Figure 5 Storage and loss moduli of PDMS at 40°C and the predictions from the relaxation spectrum of Table IV.

$$G(\gamma, t) = G(t)h(\gamma)\,(t > \tau_r) \tag{7}$$

where $G(t)$, $h(\gamma)$, and τ_r are the linear relaxation modulus, the damping function, and a material time constant that indicates the possible characteristic time of chain retraction, respectively.

The relaxation moduli of the PDMS, PMVS, and HDPE samples are shown in Figure 6. PDMS and PMVS seems to belong to the power law type, which could be attributed to the polydispersity of the samples. Similar to the data of Iza and Bousmina,[9] the modulus curves of HDPE showed slight kinks located at a time roughly independent of the strains. The corresponding damping functions [$h(\gamma_a)$'s] are shown in Figure 7. In a simplified chain entanglement network model, with the node force balance requirement taken into account, Marrucci et al.[8] proposed a new strain tensor ($\mathbf{S}$):

$$\mathbf{S} = \mathbf{C}^{-1/2}/tr(\mathbf{C}^{-1/2}) \tag{8}$$

where tr is the trace operator and $\mathbf{C}^{-1/2}$ is the square root of the Finger tensor $\mathbf{C}^{-1}$ and is deduced by the following $h(\gamma)$:

TABLE IV
Relaxation Spectrum Obtained by the Fitting of $G(t)$ of PDMS at 40°C

i	g_i	λ_i
1	3.41×10^4	1.18×10^{-2}
2	3.82×10^4	4.01×10^{-2}
3	2.15×10^4	1.81×10^{-1}
4	1.01×10^4	6.88×10^{-1}
5	2.85×10^3	2.70×10^{0}
6	2.88×10^2	1.17×10^{1}
7	3.24×10^1	1.02×10^{2}

$$h(\gamma) = \frac{6}{4 + \gamma^2 + (4 + \gamma^2)^{1/2}}, \tag{9}$$

The well-known Doi–Edwards[3] theory with the independent alignment approximation[24] gives $h(\gamma)$ as

$$h(\gamma) = \frac{1}{1 + 4\gamma^2/15} \tag{10}$$

As shown in Figure 7, when the strain was small, the experimental $h(\gamma_a)$'s agreed well with the predictions from both Doi–Edwards theory and the Marrucci model; the latter had a slight improvement over the former. The same conclusion was reported by Iza and Bousmina.[9] As the strain increased, however, the rate of strain softening predicted by the theories were considerably larger than the experimental data.

By using a straight-line-marker technique, Kaylon and Gevgilili[10,25] demonstrated that in the step strain or steady shear experiments of PDMS and HDPE, the wall slip may become a serious problem, even with a moderate level of strain. In our experiment, wall slip of the PMVS and PDMS samples was also observed for strains larger than 3, as shown in Figure 8. For the PMVS sample, we got $\gamma = 2.2$ for an apparent strain (γ_a) of 3.0 and $\gamma = 3.75$ for $\gamma_a = 5.0$; for the PDMS sample, we got $\gamma = 1.9$ for $\gamma_a = 3.0$. Thus, the wall slip could not be ignored. Another problem we confronted was flow instability or edge fracture; that is, the sample was expelled out of the plates for large strains. Reducing the gap is an effective way to enlarge the range of strain without edge fracture. In Figure 8, a relatively large gap of 1.21 mm was adopted to reveal the wall slip clearly, whereas in the experiments depicted by Figure 6, we used a small gap of 0.5 mm to reach large strains without edge fracture. It was difficult

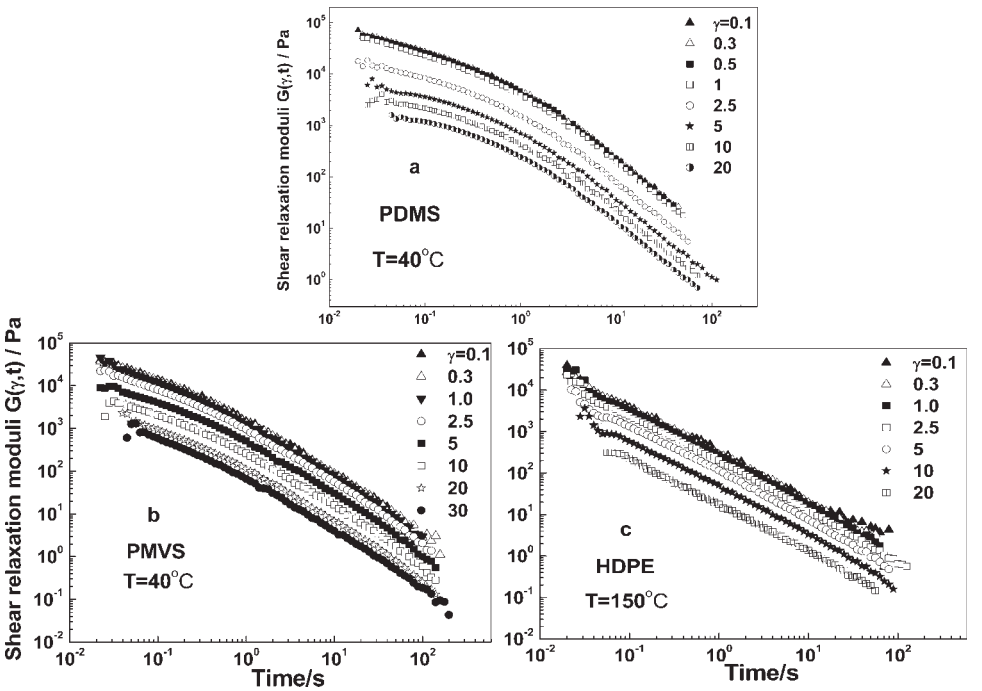

Figure 6 Stress-relaxation functions of large step strains for (a) PDMS at 40°C, (b) PMVS at 40°C, and (c) HDPE at 150°C (the strain rise time was 20–45 ms).

to determine the γ's with such a small gap by the marker technique. Fortunately, as shown in Figure 7, the slopes of $h(\gamma_a)$ for the three polymers at large strains are nearly -1, and this slope would be affected little by possible strain rectification. In fact, for a given correct stress and $G(t)$, $h(\gamma_a)$ is inversely proportional to the strain, so any strain correction on the log $h(\gamma)$–log γ plot has a slope of -1. Thus, the variation trends of the experimental $h(\gamma_a)$'s at large strains shown in Figure 7 are reliable, even though we are uncertain about the γ's.

Iza and Bousmina[9] reported good predictions of $h(\gamma)$ of the Marricci model eq. (9) for polystyrene and HDPE samples with polydispersity indicese

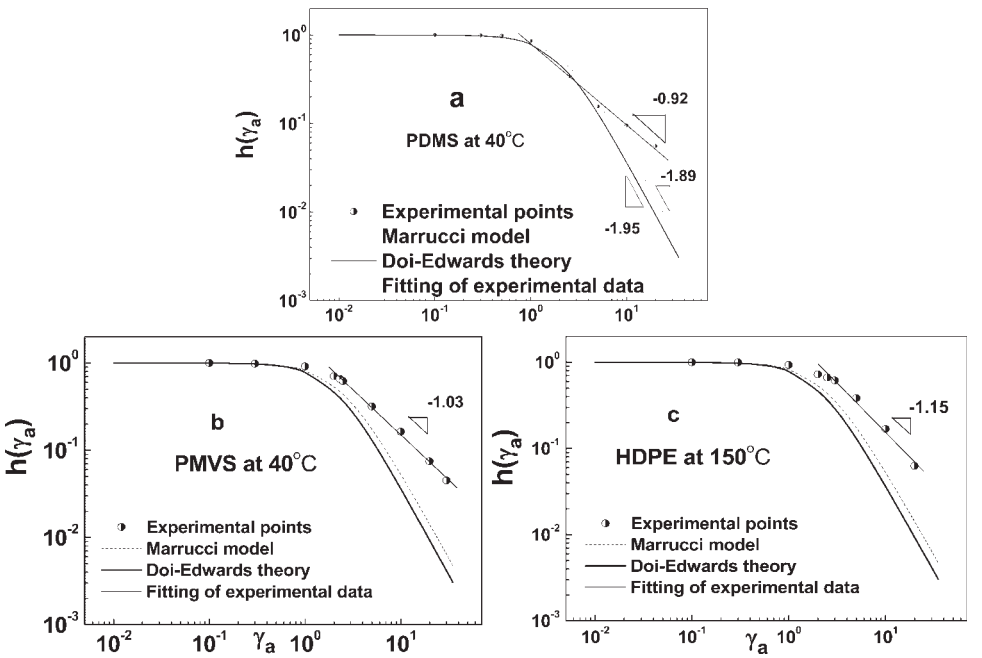

Figure 7 Comparison of the experimental damping function $h(\gamma_a)$'s with predictions of the Marrucci model and Doi–Edwards theory: (a) PDMS at 40°C, (b) PMVS at 40°C, and (c) HDPE at 150°C.

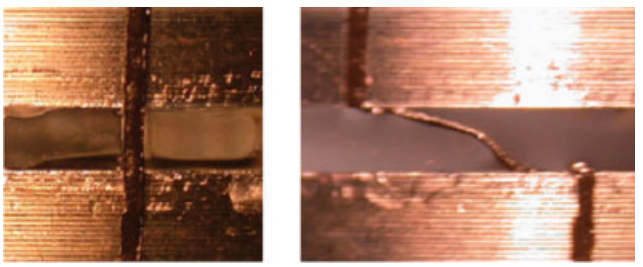

Figure 8 Wall slip as shown by a straight line marker for PMVS at 40°C in 25-mm parallel plates with a gap of 1.21 mm; γ_a was 3.0, and the strain rise time was 126 ms. [Color figure can be viewed in the online issue, which is available at www.interscience.wiley.com.]

from 1.09 to 2.45. Their maximum step strain was about 5, which was relatively low due to the fixture chosen (25-mm cone and plate) and the transducer's limit. We used 15-mm parallel plates and a 0.5-mm gap; this fixture not only enlarged the strain range but also shortened the response time of the transducer (20–45 ms) and revealed larger discrepancies of $h(\gamma)$ at larger strains between the theoretical predictions and the experiments for the three polymers with medium to large polydispersities.

Figure 9 plots the superimposed moduli via the vertical shifting of the curves in Figure 7. Generally, the time–strain separability was valid beyond a certain initial time τ_r. The determination of τ_r was arbitrary to some extent. If we took a criterion of 10% relative discrepancy of the curves, the τ_r values were 0.1, 0.06, and 0.04 s for PDMS, PMVS, and HDPE, respectively; the magnitudes were in the same order as the molecular weights. Among the three polymers, the initial time τ_r of PDMS seemed better demonstrated. If we took the initial time τ_r as a rough estimation of the Rouse time (τ_R), as suggested by Larson,[11] τ_d could be estimated by

$$\tau_d/\tau_R = M_W/M_e \tag{11}$$

where M_e and M_w are the entanglement molecular weight and weight-average molecular weight, respectively. For the PDMS sample, $M_w = 7.3 \times 10^5$, $\tau_r \approx 0.1$ s, and $M_e \approx 1 \times 10^4$, the average value from Doi and Edwards[3] and Forsman;[26] thus $\tau_d \approx 7.3$ s. According to the tube model, the strain softening is attributed to the retraction process: after a step deformation, polymer chains retract along their tube contours to their original lengths. This is accomplished in a relatively short time τ_r; the slower relaxation mechanism is the reptation of the chains to recover their isotropic orientation, which took a much longer time (τ_d). The relaxation times of the PDMS sample so far determined by various methods are summarized in Table V.

Material instability

For imposing instantaneous shear deformation, Doi–Edwards theory predicts material instability at large strains. Marrucci and Grizzuti[15] analyzed the step strain instability problem by deriving an expression

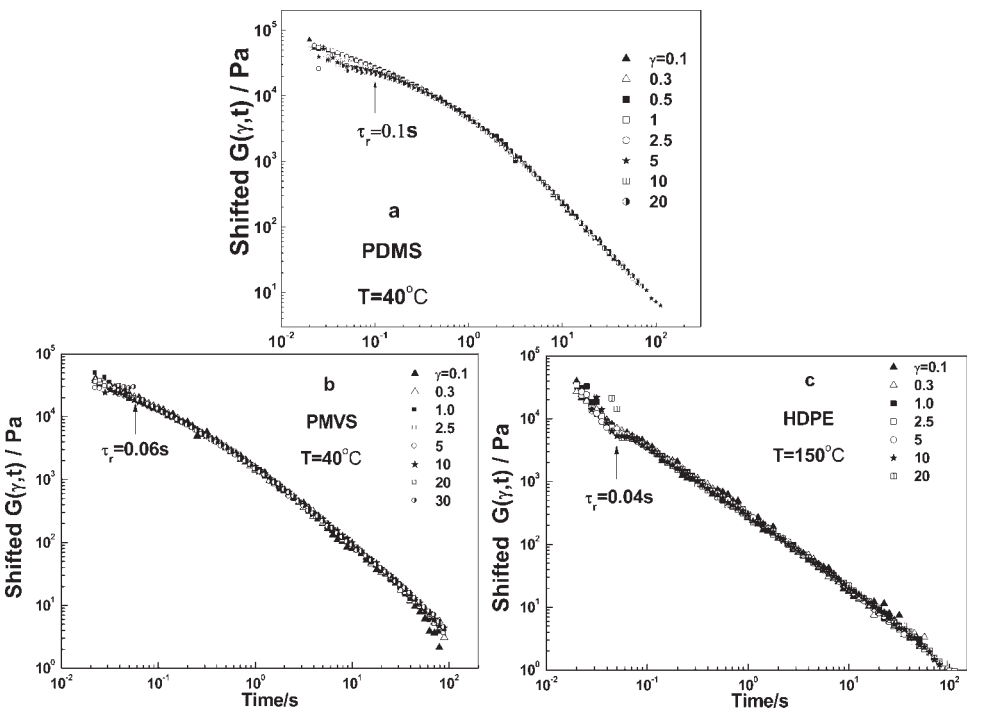

Figure 9 Superimposed relaxation modulus via vertical shifting for (a) PDMS at 40°C, (b) PMVS at 40°C, and (c) HDPE at 150°C. τ_r indicates the possible time of chain retraction.

TABLE V
Summary of the Relaxation Times of PDMS at 40°C Obtained by Various Methods

Method	Relaxation time (s)
Steady shear thinning	8.6
Dynamic shear thinning	8.2
Creep recovery	8.0
Step deformation, chain reptation	7.3
Step deformation, chain contraction	0.1
Dynamic ω_c	0.3

of deformation free energy on the basis of the reptation model with independent alignment approximation. The curve of free energy versus shear strain has an inflection point at a strain of $\gamma_m \approx 2.1$, which corresponds to a maximum of stress in the stress–strain relations. Deformation beyond the inflection point is unstable, and not only that, deformation before the inflection point is possibly metastable: perturbations may have caused the sample to split into two layers of smaller and larger strains, respectively, which satisfied the assigned strain but with smaller total free energy. Later, Marrucci et al.[8] proposed a simplified form of the free energy derived from the orientation tensor of eq. (8), and the maximum of stress for an instantaneous shear deformation took place at $\gamma_m \approx 2.3$.

As shown in Figure 8, a kink was observed on the marker line, which implied that the bulk deformation may have been nonuniform in addition to the wall slip. In Figure 10, we present τ versus the apparent step strain at various instances when the target strains were just reached. The shear stresses (τ's) of PDMS, PMVS, and HDPE exhibited peaks at strains of 1.0, 2.5, and 3.0, respectively. Moreover, the second peaks of the τ's appeared at strains of 15, 20, and 20, respectively. However, one must bear in mind that the large strains after the stress peak corresponded to unstable states, and wall slip or stratification may have already occurred in the samples.

Elastic stresses (τ''s) of the step deformation and oscillatory shear at large strains

When the strain amplitude of an oscillatory shear flow is small, the storage and loss moduli represent the elastic and viscous natures of the sample, respectively. For LAOS, the stress curve as a function of time cannot be described by a single trigonometric function; thus, the dynamic moduli reported by the rheometer no longer adequately represent the elastic and viscous contributions. Recently, on the basis of the stress symmetry of LAOS, Cho et al.[19] proposed a new method to decompose the stress response into elastic and viscous parts. The decomposition method is described as follows.

If $\gamma(t)$, $\dot{\gamma}(t)$, and ω are the shear strain, shear rate, and angular frequency, respectively, let

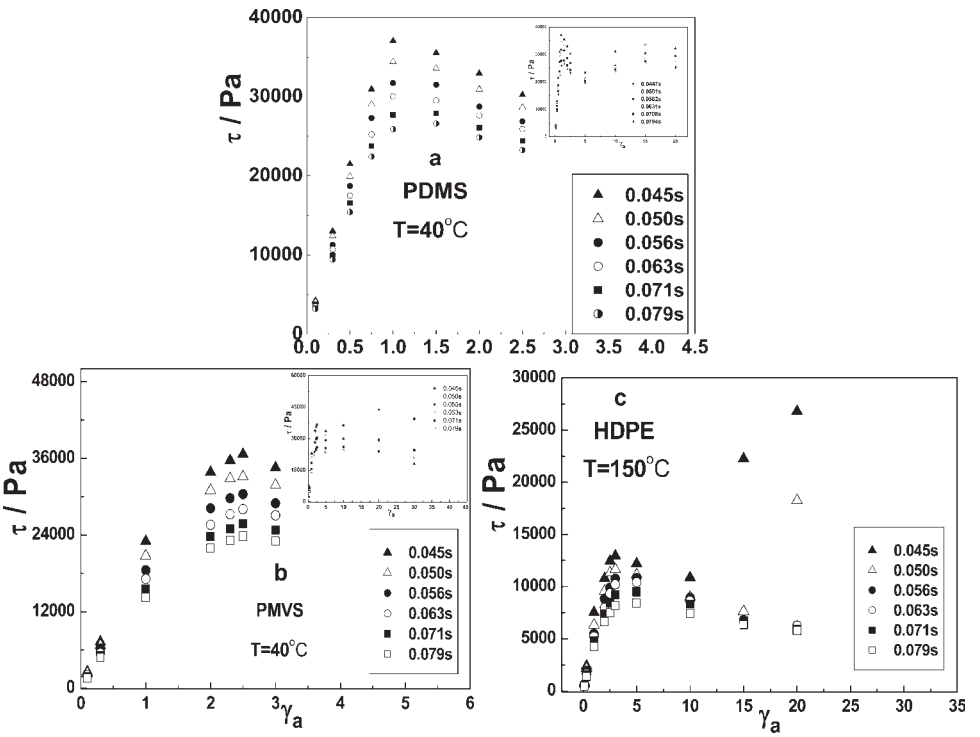

Figure 10 Stresses at different moments versus the apparent step strain for (a) PDMS at 40°C, (b) PMVS at 40°C, and (c) HDPE at 150°C. The strain rise times were 20–45 ms. The insets show the stress–strain curves in the whole range of strains.

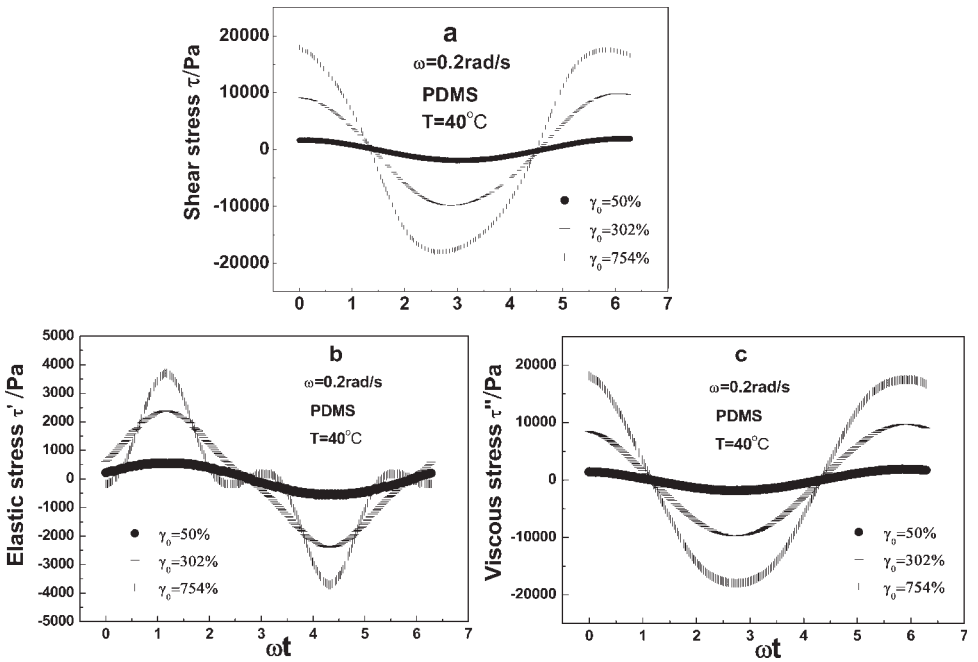

Figure 11 Total elastic and viscous shear stresses of PDMS at 40°C with a frequency of 0.2 rad/s and strain amplitudes of 0.5, 3.02, and 7.54, respectively.

$$x = \gamma \text{ and } y = \dot{\gamma}/\omega \tag{12}$$

The shear stress (τ) is an odd function for both strain and shear rate, that is

$$\tau(-x,-y) = -\tau(x,y) \tag{13}$$

Thus, τ can be decomposed as

$$\tau(x,y) = \frac{\tau(x,y) - \tau(-x,y)}{2} + \frac{\tau(x,y) - \tau(x,-y)}{2} \tag{14}$$

The first term on the right-hand side of eq. (14) is odd for x and even for y, and the second term is even for x and odd for y. Considering the work consumption characteristics in cyclic deformation, Cho et al. defined the elastic stress (τ') and viscous stress (τ'') as

$$\tau' = \frac{\tau(x,y) - \tau(-x,y)}{2}, \tau'' = \frac{\tau(x,y) - \tau(x,-y)}{2} \tag{15}$$

Figure 11 shows an example of the stress decomposition for the PDMS sample at 40°C for three strain amplitudes at $\omega = 0.2$ rad/s; the linear regime was $\gamma_0 < 0.8$, as determined by a strain sweep. At the small strain $\gamma_0 = 0.5$, the elastic waveforms was basically sinusoidal; at the moderate strain $\gamma_0 = 3.02$, τ' deviated a little from the sinusoidal function; and at the large strain $\gamma_0 = 7.54$, the τ' waveform was distorted heavily with an additional peak–valley. On the other hand, the τ'' waveforms always seemed close to sinusoidal functions. This behavior was first observed by Cho et al.[19] for polypropylene at $\omega = 1$ rad/s and 170°C. At large strains, the total shear stress amplitude (τ_{max}) dropped gradually as the oscillatory shearing proceeded. Hatzikiriakos and Dealy[27] attributed the attenuation of stress amplitude in LAOS to the wall slip, which did not occur instantly but evolved with slip relaxation time. Here, to avoid the complexity of the wall slip relaxation, we concentrated on the first few cycles and applied Cho et al.'s decomposition method to the stress waves as soon as they were symmetric.

In the stress relaxation experiment, the time interval for the application of target strain was very short (20–45 ms), so the response could be taken as the initial buildup of τ' and its later relaxation. In the linear viscoelastic regime, $G(t)$ and $G'(\omega)$ are related by eq. (4), which held for this PDMS sample, as shown in Figure 4. It is interesting to check this relation in the nonlinear regime. For the purpose, the generalized dynamic moduli defined by Cho et al.[19] were used:

$$G'_N(\omega,\gamma_0) = \tau'_{max}/\gamma_0,\ G''_N(\omega,\gamma_0) = \tau''_{max}/\gamma_0 \tag{16}$$

where γ_0 is the strain amplitude and $G'_N(\omega,\gamma_0)$ is the generalized storage modulus and τ_{max}' and τ''_{max} are the decomposed maximum τ' and τ'' in a cycle, respectively. In Figure 12, we compare $G(\gamma,t)$ and $G'_N(\omega,\gamma_0)$ for the PDMS sample on the timescale $t = 1/\omega$. Both the moduli exhibited softening at large strains. As ω increased from 0.2 to 5.0 rad/s, the difference between $G(\gamma,t)$ and $G'_N(\omega,\gamma_0)$ became smaller

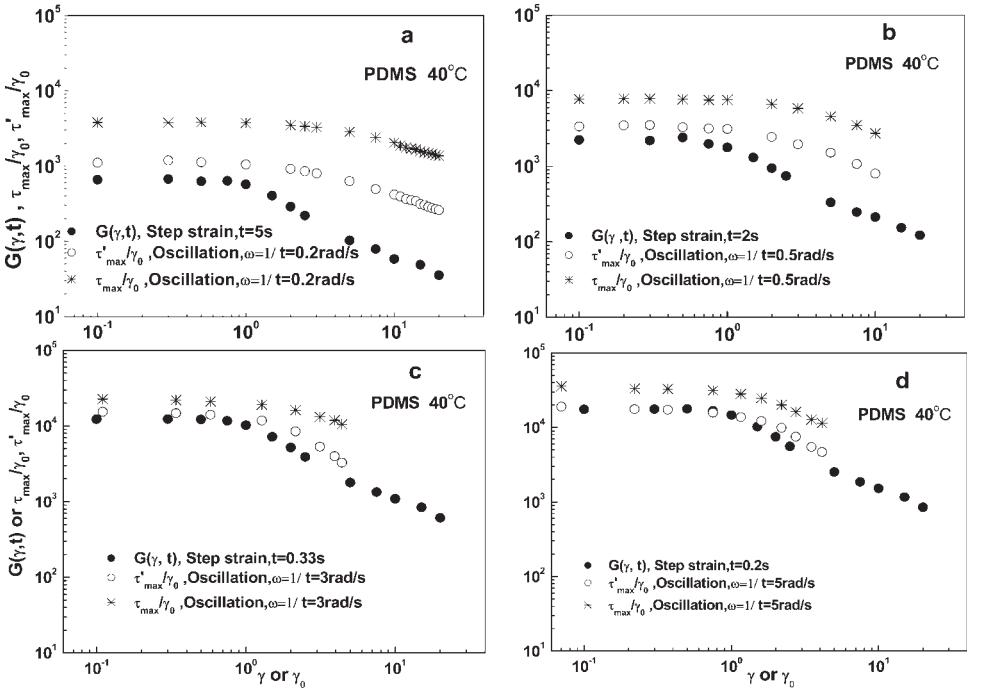

Figure 12 Comparison of generalized moduli [τ_{max}/γ_0 and τ'_{max}/γ_0] in oscillatory shear to $G(\gamma,t)$ in the step deformation of PDMS at $t = 1/\omega$ and 40°C.

and smaller, whereas τ_{max} remained considerably larger than τ'_{max}. At the lower frequencies of 0.2 and 0.5 rad/s (the linear regime was $\gamma_0 < 0.7$), the two moduli diverged as the strain entered into the nonlinear regime of $G(\gamma,t)$, but at the higher frequencies of 3 and 5 rad/s (the linear regime was $\gamma_0 < 0.22$), $G'_N(\omega,\gamma_0)$ approached $G(\gamma,t)$, even in the nonlinear regime. The edge fracture problem prevented our LAOS experiment from further increasing ω.

CONCLUSIONS

The characteristic relaxation times of a PDMS sample with medium polydispersity were measured by various rheological tests. Compared with the linear relaxation spectrum, the obtained characteristic times at 40°C formed two groups: one corresponded to the chain reptation relaxation (≈8 s), and the other corresponded to the chain retraction relaxation (≈0.1 s, roughly τ_R). The crossover frequency (ω_c) of G' and G'' seemed to belong to the latter.

In the step shear deformation experiment, the relaxation behavior of the medium polydisperse PDMS and PMVS samples belonged to the power law type, whereas that of the highly polydisperse HDPE sample belonged to the kinked type. In terms of damping function ($h(\gamma)$), the Doi–Edwards theory and Marrucci model overestimated the strain softening for the three commercial polymers. The occurrence of stress peaks in the step deformation experiment as the strain increased above a critical value was detailed, which implied possible strain localization or stratification in the samples. The critical strains were about 1.0, 2.5, and 3.0, respectively, close to the predictions of 2.1 and 2.3 by Doi–Edwards theory or the Marrucci model, respectively.

The elastic and viscous stress (τ' and τ'') decomposition method proposed by Cho et al.[19] was applied to the data of LAOS of the PDMS sample. As ω increased, $G'_N(\omega,\gamma_0)$ approached the relaxation modulus at the timescale $t = 1/\omega$ in both the linear and initial nonlinear regimes.

References

1. Eirich, F. R. Science and Technology of Rubber; Academic: New York, 1978.
2. Ferry, J. D. Viscoelastic Properties of Polymers, 3rd ed.; Wiley: New York, 1980.
3. Doi, M.; Edwards, S. F. The Theory of Polymer Dynamics; Clarendon: Oxford, 1986.
4. Awati, K. M.; Park, Y.; Weisser, E.; Mackay, M. E. J Non-Newtonian Fluid Mech 2000, 89, 117.
5. Elmoumni, A.; Winter, H. H.; Waddon, A. J.; Fruitwala, H. Macromolecules 2003, 36, 6453.
6. Mark, J.; Ngai, K.; Graessley, W.; Mandelkern, L.; Samulski, E.; Koenig, J.; Wignall, G. Physical Properties of Polymers, 3rd ed.; Cambridge University Press: Cambridge, 2004.
7. Osaki, K. Rheol Acta 1993, 32, 429.
8. Marrucci, G.; Greco, F.; Ianniruberto, G. Macromol Symp 2000, 158, 57.
9. Iza, M.; Bousmina, M. Rheol Acta 2005, 44, 372.
10. Gevgilili, H.; Kaylon, D. M. J Rheol 2001, 45, 467.
11. Larson, R. G. The Structure and Rheology of Complex Fluids; Oxford University Press: New York, 1999.

12. Archer, L. A.; Chen, Y. L.; Larson, R. G. J Rheol 1995, 39, 519–525.
13. Tapadia, P.; Wang, S. Q. Phys Rev Lett 2006, 96, 016001–1.
14. Tapadia, P.; Wang, S. Q. Phys Rev Lett 2006, 96, 196001–1.
15. Marrucci, G.; Grizzuti, N. J Rheol 1983, 27, 433.
16. Papanastasiou, A. C.; Scriven, L. E.; Macosko, C. W. J Rheol 1983, 27, 387.
17. Graham, M. D. J Rheol 1995, 39, 697.
18. Hyun, K.; Kim, S. H.; Ahn, K. H.; Lee, S. J. J Non-Newtonian Fluid Mech 2002, 107, 51.
19. Cho, K. S.; Hyun, K.; Ahn, K. H.; Lee, S. J. J Rheol 2005, 49, 747.
20. Chen, Q.; Fan, Y. R.; Zheng, Q. Rheol Acta 2006, 46, 305.
21. Nielsen, L. E. Polymer Rheology; Science Press: China, 1983.
22. Baumgaertel, M.; Winter, H. H. Rheol Acta 1989, 28, 511.
23. Macosko, C. W. Rheology Principles, Measurements, and Applications; Wiley: New York, 1994.
24. Laun, H. M. Rheol Acta 1978, 17, 1.
25. Kaylon, D. M.; Gevgilili, H. J Rheol 2003, 47, 683.
26. Forsman, W. C. Polymer in Solution: Theoretical Considerations and Newer Methods of Characterization; Plenum: New York, 1986.
27. Hatzikiriakos, S. G.; Dealy, J. M. J Rheol 1991, 35, 497.